Eur. Phys. J. B **7**, 393–400 (1999)

THE EUROPEAN PHYSICAL JOURNAL B

EDP Sciences

Orientational diffusivities measured by Rayleigh scattering in a lyotropic calamitic nematic (N_C) liquid crystal phase: the backflow problem revisited

M.B. Lacerda Santos[a] and M.A. Amato

Instituto de Física, Universidade de Brasília, 70910-900 Brasília, DF, Brazil

Received: 29 April 1998 / Revised: 19 August 1998 / Accepted: 31 August 1998

Abstract. Using a light-beating technique we have measured the damping time of thermal fluctuations of the nematic director for the so called cylindrical or calamitic nematic (N_C) phase of the lyotropic system K-laurate/decanol/D_2O. By varying the scattering angle in suitable geometries, we have been able to estimate the orientational diffusivities associated to the three pure deformations of splay, twist and bend. A former measurement made in the disk-like N_D phase of the same system yielded a large deviation between the splay and twist diffusivities. The effect was then attributed to induced flows, or backflow, which could be responsible for the reduction of the splay viscosity. In fact, this is the analogous effect, for disks, to the one recognized since long time ago arriving for rod-like molecules in a classical nematic, though in this case it is associated with bend deformations. The analogy comes about thanks to the interchange of the role played by disks and cylinders for, respectively, splay and bend fluctuations.The measurements reported here provide a new test on the applicability of the backflow model to a nematic system composed of micelles, that is, aggregates made of amphiphilic (surfactant) molecules, in its cylindrical-like variant, *i.e.* the N_C phase. In addition, the comparative study made here with the previous results existing in the literature for the N_D phase, allows us to conjecture on structural issues concerning lyotropic nematics.

PACS. 77.84.Nh Liquids, emulsions and suspensions; liquid crystals – 61.30.Gd Orientational order of liquid crystals; electric and magnetic field effects on order – 78.35.+c Brillouin and Rayleigh scattering; other light scattering

1 Introduction

Thermal fluctuations of the orientational director are a basic property of nematic liquid crystals, as well as the strong scattering of light they give rise to. Let $\mathbf{n}_o$ be the unit vector specifying the average direction of alignment, that is, the optical axis. Following de Gennes [1], the fluctuations of the local director $\mathbf{n}$ may be expressed in terms of normal modes parallel and perpendicular to the plane defined by $\mathbf{n}_o$ and a given wavevector $\mathbf{q}$, according to

$$\mathbf{n} = \mathbf{n}_o + \delta n_1\, \mathbf{e}_1 + \delta n_2\, \mathbf{e}_2. \tag{1}$$

Here δn_1 is the mode made of a combination of splay and bend deformations, while the mode δn_2 combines twist and bend, see Figure 1. The director fluctuations have characteristic relaxation or damping rates, Γ, and since long ago [2], photon correlation techniques have been used to measure them. Such measurements yield informations about elastic and viscous properties of the nematic system, as Γ is given by

$$\Gamma_i = \frac{1}{\eta_i(\mathbf{q})}(K_i q_\perp^2 + K_3 q_\parallel^2), \tag{2}$$

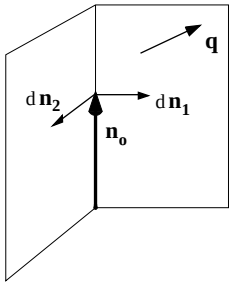

Fig. 1. Defining the nematic director fluctuation modes 1 and 2.

where $i = 1, (2)$ labels the above defined fluctuation modes, while $q_\parallel$ ($q_\perp$) is the component of the scattering wavevector $\mathbf{q}$ parallel (normal) to the optical axis. K_1, K_2 and K_3 are the Frank elastic constants characterising, respectively, splay, twist and bend deformations.

Some particular scattering geometries lead to simpler formulas. For instance, for $\mathbf{q} \perp \mathbf{n}_o$ (see Fig. 2), pure deformations of twist can be probed for depolarised scattering,

[a] e-mail: mbls@guarany.cpd.unb.br

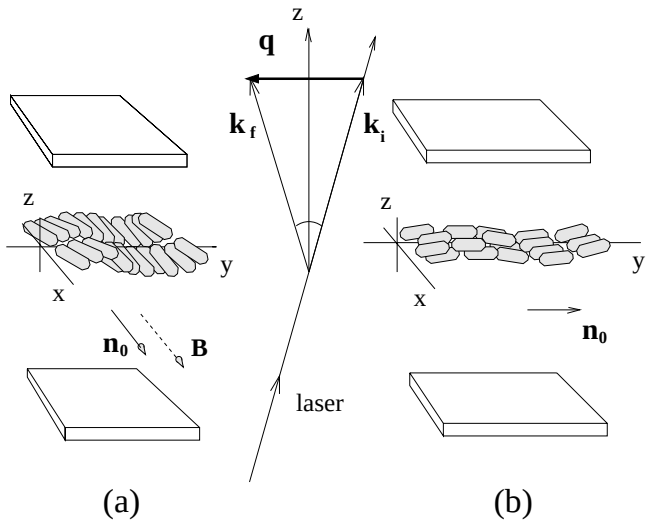

Fig. 2. Schematics of the two geometric configurations used for depolarised scattering and the corresponding fluctuation types probed with: (a) the nematic director $\mathbf{n}_o$ of the N_C phase is previously oriented by a magnetic field of 5 kG along the x-axis, which is defined by the normal to the scattering plane: damping rates are then measured for twist. (Splay fluctuations are probed in polarised scattering – see text); (b) the sample is rotated of 90° around the z-axis, which allows measuring the damping rate for bend fluctuations (for both polarizations).

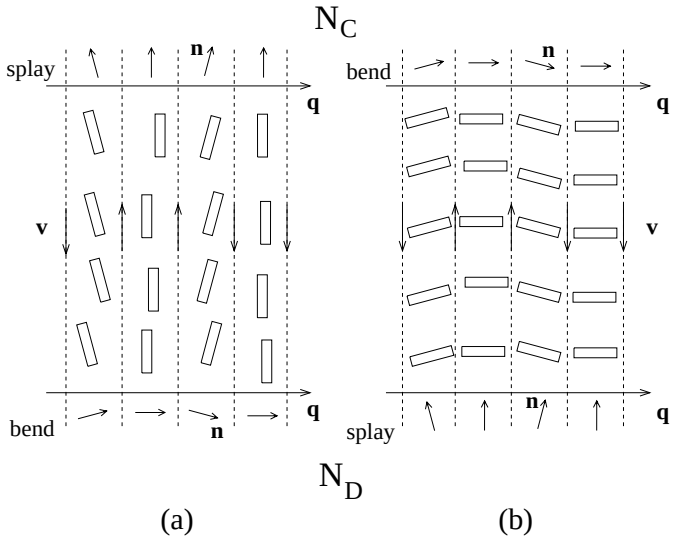

Fig. 3. Disks or cylinders? Two-dimensional side view of idealised micelles illustrates the interchange of the role played by disks and cylinders concerning the backflow mechanism in the two types of uniaxial nematic phases: the coupling between order and flow is expected to be stronger in the situation depicted in (b) than in (a), that is, for bend fluctuations in the N_C phase and for splay fluctuations in the N_D phase.

giving

$$\Gamma_{twist} = \frac{K_2}{\eta_{twist}}\, q^2 \equiv D_{twist} q^2, \qquad (3)$$

where $\eta_{twist} \equiv \gamma_1$ is the rotational viscosity coefficient [1]. Indeed, by exploring other suitable geometries and polarisations, light beating measurements can give access to the so called diffusivities D_{splay}, D_{twist} and D_{bend}, which are given by simple formulas as in equation (3), that is, an elastic constant divided by a viscosity coefficient.

For most materials, elastic constants show a relatively weak anisotropy. However, the situation is different for the viscosity coefficients. For classical thermotropic nematics, *i.e.*, pure systems made of elongated molecules, it is well-known [1] that one usually has $\eta_{bend} \ll \gamma_1$. This result can be explained in terms of the nematodynamics equations thanks to a backflow effect [1], which means that induced flows assist the bend fluctuations of the elongated rods, reducing the internal dissipation. In principle, the splay fluctuations would also benefit of a reduction on its associated friction coefficient, but the shape anisotropy actually makes such a reduction negligible [3].

The subsequent appearance of lyotropic nematics, which are made of amphiphilic aggregates or micelles, brought new ingredients to the matter. They present not a single but two types of uniaxial nematic phases: one "cylindrical like" – uniaxially positive – and the other "disk-like" – uniaxially negative, hereafter denoted by N_C and N_D, respectively. For the N_D phase, light scattering measurements gave [3] $D_{splay} \gg D_{twist}$ by a factor of about seven. Arguing that the deviation between the corresponding elastic constants could barely goes beyond a factor of two or three, the authors concluded that this result implies on $\eta_{splay} \ll \gamma_1$, that is, the lyotropic N_D phase shows a reversed behaviour, in comparison to the one shown by a classical thermotropic nematic.

In the same paper [3], the authors explained this reversal between splay and bend in terms of the interchange of the role played by disks and cylinders in each one of the two kinds of uniaxial nematic phases. That is, splay in N_D "looks like" bend in N_C (see Fig. 3). The backflow mechanism is explained in the quoted paper, on the basis of the nematodynamics equations. Further discussion of this problem appeared later in the literature, in connection with morphological instabilities [4]. However, the basic idea can be easily understood with help of Figure 3, that makes an appeal to the fact that the two kinds of objects appear identical in side view. It is hoped that such an intuitive approach suffices for the purposes of the present discussion.

Although the backflow model provides a satisfactory explanation for most of the known diffusivity data, a recent light-scattering experiment performed with a thermotropic discotic phase [5] did not reproduce the expected effect. We shall come back to this result later.

In this paper we report light-scattering measurements of characteristic times of thermal fluctuations of the nematic director in a so called cylindrical or calamitic nematic (N_C) phase of the lyotropic system K-laurate/decanol/heavy water (referred hereafter as LDhW, for short). The relative concentrations were

chosen in order to have a large temperature range for the N_C phase, and the measurements were performed far from phase transitions. The measurements were taken as a function of the scattering angle in suitable geometries, in order to determine the orientational diffusivities associated to the three pure deformations of splay, twist and bend.

The denomination "cylindrical" originates from a conventional interpretation of structural data [6], according to which the N_C phase would be composed of elongated micelles, being thus the lyotropic counterpart of the classical thermotropic nematic. Although part of the measurements presented here can be compared with ones made in reference [7], this is, to our knowledge, the first complete characterisation of director fluctuations in the N_C phase, that is, by issuing diffusivity coefficients for splay, twist and bend fluctuations.

The paper is organised in four sections. The first is the introduction, and the second, contains a description of the experimental methods. Then, in the third part, we present the results and their analysis. This shows that the lyotropic N_C phase behaves as expected when the backflow model is applied to classical nematic materials made of rigid-rod molecules. Specifically, it is shown that $D_{bend} \gg D_{twist}$, and $D_{splay} \approx D_{twist}$. Finally, in the fourth section we present the conclusions by discussing the relationship of these data for the N_C phase and the previous ones for the N_D phase. Then, we show that the study of the backflow phenomena may lead to inferences about the shape of the elementary objects that constitute these different types of liquid crystal phases. As all conventional techniques of structural determinations (X-rays, neutron scattering) suffer of being subjected to long time averaging processes, dynamical information provided by backflow, although indirect, may become very helpful.

2 Experimental

The lyotropic liquid crystal we use [8] and the procedures for sample preparation as well as the light beating technique are essentially the same as in previous publications [7,9], and will be only briefly described here. The lyotropic phase is prepared by mixing potassium laurate (purified by recrystallization), 1–decanol (> 99%, from Fluka) and D_2O (Sigma) in the weights proportions 25.80 per cent, 6.20 per cent and 68.00 per cent, respectively. The mixture is sealed in a Pyrex tube, homogenised by vigorous shaking combined with centrifugation and then left at rest for several weeks.

Just before filling a light scattering cell, the lyotropic mixture is submitted to further centrifugation for one hour at 4000 rpm to sediment dust. Care must then be taken so to pipette the lyotropic phase only from the upper part of the tube. The liquid is then transferred into a Hellma cell made of two circular glass plates separated by a 1 mm thick glass spacer, the whole being assembled by a specially designed mounting system allowing high compression of the plates. This system practically eliminates water loss problems verified in earlier works [3,7]. All glass surfaces were previously thoroughly cleaned (with strong detergent) and rinsed in hot deionized distilled water.

Next, the sample cell is placed with its plates lying horizontally in an oven in thermal contact with a circulating heat bath, controlled so that the long term thermal stability (1 h) is better than 0.1 °C. The sample temperature is monitored with help of a chromel-constantan thermocouple.

The lyotropic mixture used here exhibits a calamitic (or cylindrical-like) nematic N_C phase in the temperature range from 8 °C to 49 °C. At higher temperatures, the system exhibits a fluid milky phase, while the low temperature neighbouring phase is a viscous and birefringent one (possibly a hexagonal phase). Whatever the exact nature of these neighbouring phases are, after getting on them, the N_C phase can readily be recovered by simple adjustment of the temperature in the appropriate range. All measurements here have been taken at a fixed temperature of 29.4 °C.

The N_C phase has a positive diamagnetic anisotropy and so a magnetic field parallel to the glass plates, combined with wall effects provided by them, can yield a homogeneous alignment of the director. In our experiment, a magnetic field of about 5 kG, provided by a 6 in. magnet (Newport) has been periodically applied to the sample, during several hours. The sample was not kept under influence of the field during the measurement runs. However, the quality of the alignment was checked optically before and after each run, and it remained usually good much longer than the necessary time.

Figure 2 schematises the scattering geometry. A HeNe 35 mW laser (Spectra Physics, mod. 127) beam oriented along $\mathbf{k}_i$ traverses the sample cell making an (internal) angle of $\theta/2$ with respect to the glass plate normal (z-axis). The selection of the scattered wave vector $\mathbf{k}_f$ direction follows an optical alignment procedure that uses the reflected beam from the cell, yielding the symmetrical geometry of Figure 2 and enabling a precise definition of the scattering plane (y, z). The direction of $\mathbf{n}_o$ follows $\mathbf{B}$ and is made perpendicular to the scattering plane within an error of $\sim 2°$. As $|\mathbf{k}_i| \approx |\mathbf{k}_f|$, due to the low birefringence of lyotropic nematics ($\Delta n \sim 10^{-3}$), this results in $\mathbf{q}$ parallel to the $y-$axis. In order to calculate $|\mathbf{k}|$ we used a (mean) refractive index of $n = 1.38$, which was determined for a lyotropic mixture of neighbouring concentrations [3]. The three values of q used in the experiment are, in units of 10^6 m^{-1}: $q_1 = 2.08$, $q_2 = 3.49$, and $q_3 = 4.44$.

The incident polarisation vector $\mathbf{i}_o$ is made parallel to the scattering plane by a Nicol prism regulated within better than 0.5°. A polarizer sheet is used to define the polarisation of the scattered beam parallel or perpendicular to the scattering plane for the ordinary ($\mathbf{f}_o$) and extraordinary ($\mathbf{f}_e$) polarisations, respectively. For the "depolarised" configurations (either (o, e) or (e, o)), the geometry of Figure 2a, with $\mathbf{q} \perp \mathbf{n}_o$, provides optical coupling with mode 2 giving pure twist deformations. Thus, as seen in equation (3), the damping rate of the fluctuations turns out

to be simply,

$$\Gamma_{twist} = \frac{K_2}{\gamma_1}\, q^2. \tag{4}$$

The selected scattered light beam is then collected by a pinhole with opening area $A \ll A_c$, where A_c is the coherence area [10], and then focused on to the photocathode of the photomultiplier tube (ITT, mod. FW-130). The whole optical setup is assembled on a heavy bench floating on pneumatics to prevent from mechanical vibrations. Detailed information about our light beating spectrometer has been given elsewhere [11].

The output pulses of the photomultiplier are square shaped by a pre-amplifier discriminator (PAR 1182) and then sent to the photon correlator. A detailed description of our software correlator has been published elsewhere [12]. Here, we only mention that it uses 14 bit registers, which turns out to be much more suitable to handle with slow signals (< 10 Hz) than the conventional 4 bit correlators. Indeed, so large registers prevent attenuation of the optical signal during long time scales, allowing more rapid accumulation of the data.

Finally, the accumulated autocorrelation function is then fitted, according to the case, to a single or double exponential function with a free baseline, *i.e.*, the functions,

$$y = A_1 \exp(-t/\tau_1) + B, \tag{5}$$

of three adjustable parameters (A_1, τ_1 , and B) or,

$$y = A_1 \exp(-t/\tau_1) + A_2 \exp(-t/\tau_2) + B, \tag{6}$$

of five adjustable parameters (A_1, A_2, τ_1, τ_2 and B). This second form raises the question about the origin of the long-time component of the signal. In fact it can be various – micellar, hydrodynamic perturbations, *etc.* – and will not concern us here [9].

A word is worth saying about a (rather technical) point concerning the optical detection. At the low angles used in our experiment ($\theta < 20°$), the signal tends to be a pure heterodyne one, *i.e.*, the result of the optical beating between the "physical" (dynamical) signal and the "local oscillator" (static signal due to, *e.g.*, micro defects). (For the fundamental concepts of the light beating spectroscopy we refer the interested reader to the book by Berne and Pecora [10].) However, as we are interested mainly in depolarised light signals, a small mixture with homodyne signal may occur. The main difference is that a (single exponential) homodyne signal has exactly one half of the characteristic time of its heterodyne version. The trouble here is that a two-exponential fit is unable to resolve the two components. Fortunately, a weak homodyne component can be related to ratio between the signal intensity and the baseline, *i.e.*, $R = A_1/B$. A few of our autocorrelation functions presented such a component. To correct these data (typically within $\sim 10\%$) we used a numerical technique explained in reference [13], which yields a R dependent correction factor plotted in Figure 4.

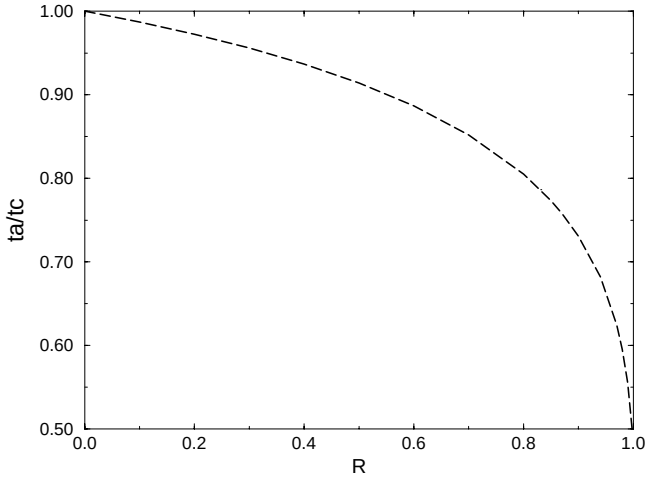

Fig. 4. "Abacus" for determining an eventual weak homodyne contribution in the autocorrelation spectra, according to reference [13] (see text).

Before ending this section, let us mention that a number of experimental difficulties tend to limit the accuracy of the measurements. We refer the interested reader to reference [9] for a discussion about these matters.

3 Data analysis and results

Figures 5 to 8 show examples of autocorrelation functions illustrating different aspects of the experiment.

Specifically, Figure 5 is a depolarised signal obtained in the "twist geometry" (of Fig. 2a) for $q_3 = 4.44 \times 10^6\,\mathrm{m}^{-1}$, fitted in (a) with the one exponential formula of equation (5) with parameter values $A_1 = 3.56 \times 10^4$, $\tau_1 = 0.299\,\mathrm{s}$ and $B = 1.68 \times 10^5$. An improved fit of this signal appears in (b), where the two-exponential formula (6) was used, with the following parameters: $A_1 = 2.62 \times 10^4$, $\tau_1 = 0.157\,\mathrm{s}$, $A_2 = 2.59 \times 10^4$, $\tau_2 = 1.54\,\mathrm{s}$ and $B = 1.55 \times 10^5$.

The depolarized spectrum of Figure 6 was also obtained for the same wavevector, but after rotating the sample of 90° around the vertical axis (with $\mathbf{B} = 0$, see "bend geometry", of Fig. 2b). The two exponential fit (with parameters: $A_1 = 6184$, $\tau_1 = 3.36 \times 10^{-3}$ s, $A_2 = 2024$, $\tau_2 = 0.19\,\mathrm{s}$ and $B = 9.68 \times 10^4$) features a short time component, characteristic of bend fluctuations in the N_C phase.

Refering to Figure 6, note the dramatic loss in the quality of the signal. This could indicate a strengthening of the elastic constant associated to bend distortions. Although this hypothesis requires an independent measurement to be fully tested, it is also suggested by Figure 7. Here, the signal also comes from bend fluctuations, but for the smallest wavevector used, $q_1 = 2.08 \times 10^6\,\mathrm{m}^{-1}$. In spite of the low angle, which favours high scattered intensity, the signal is rather noisy.

Occasionally, a small homodyne contribution may occur for spectra of depolarised light at higher angles. Typically, the short time component of such signals gave

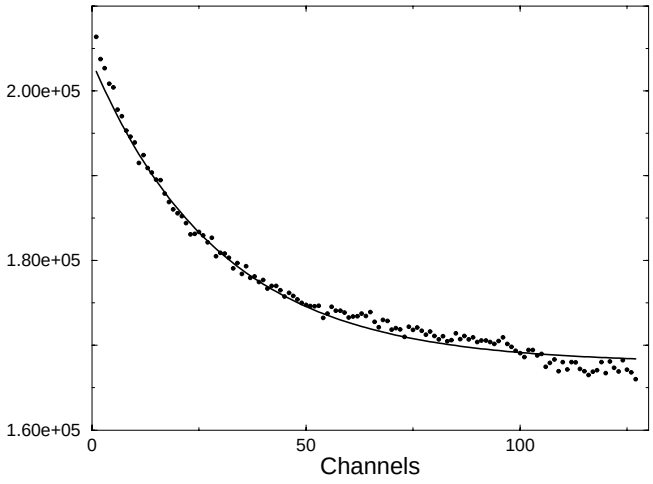

(a)

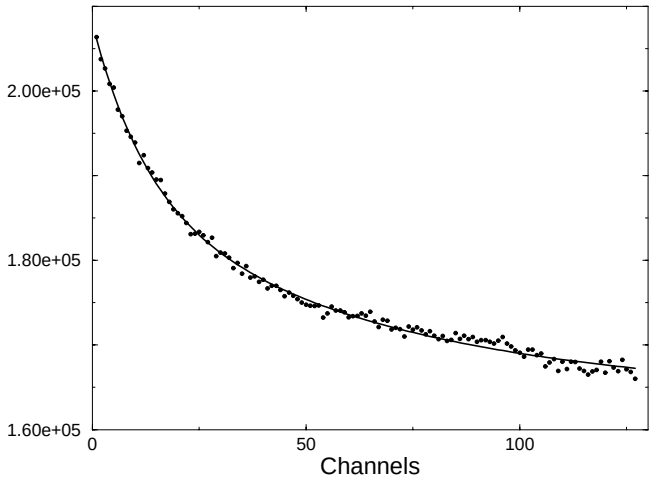

(b)

Fig. 5. Example of depolarized light signal obtained in the "twist configuration" of Figure 2a fitted with (a) one exponential and (b) two exponentials (wavevector: $q_3 = 4.44 \times 10^6\,\mathrm{m}^{-1}$; time scale: $\Delta\tau = 10$ ms).

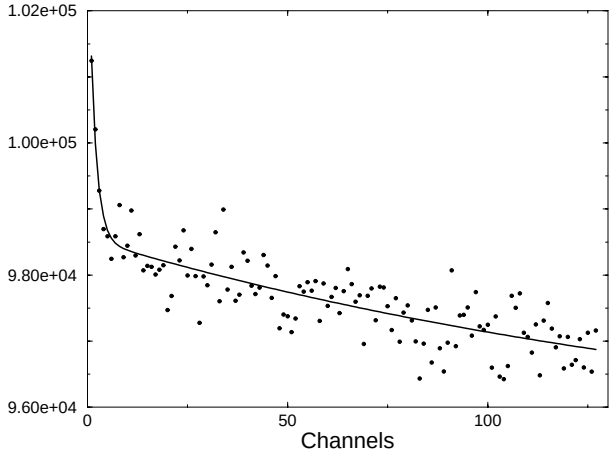

Fig. 6. Example of depolarised signal obtained after rotating the sample ("bend configuration" of Fig. 2b). The two exponential fit features a short time component, characteristic of bend fluctuations in the N_C phase ($\Delta\tau = 3$ ms, same wavevector).

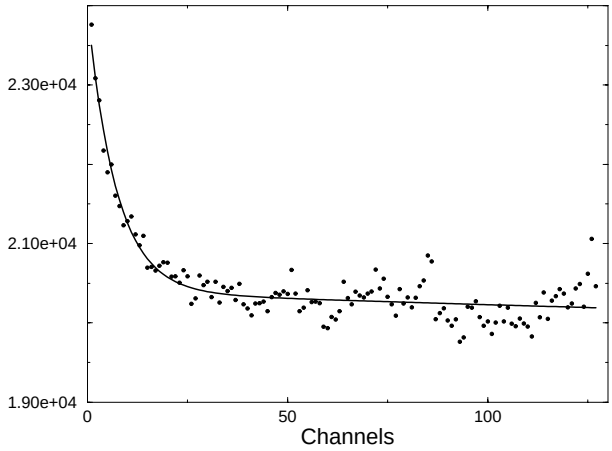

Fig. 7. *Idem*, but for the lowest wavevector used, $q_1 = 2.08 \times 10^6\,\mathrm{m}^{-1}$ ($\Delta\tau = 3$ ms).

a A_1/B ratio ranging between 0.1 and 0.4. As it was discussed in the experimental section, whenever this arrived, the corresponding decay times were corrected (for a few percent), using the graphical "abacus" of Figure 4.

As a final example of typical spectra, Figure 8 shows a polarised spectrum obtained in a geometry similar to that of Figure 2a but in the polarisation configuration extraordinary -to- extraordinary (e, e). Rigorously speaking, this symmetrical geometry leads to the extinction of the light scattering signal, according to a well-known selection rule [1]. However, a weak signal is still obtained due to small imperfections in the sample alignment [3]. In the context of a model of rigid rod particles, it is not difficult to show that the residual signal involves a mixture of splay and twist. Of course, here we have in addition the ever present long-time component, mentioned in Section 2. The example shown in Figure 8 corresponds to the wavevector $q_2 = 3.49 \times 10^6\,\mathrm{m}^{-1}$, and was also fitted with help of equation (6) for the parameter values $A_1 = 1.31 \times 10^4$, $\tau_1 = 0.718$ s, $A_2 = 1.26 \times 10^4$, $\tau_2 = 2.70$ s and $B = 1.798 \times 10^6$.

Now we proceed to the systematic analysis of the whole set of data. Figure 9 shows the plot for the low branch of "frequencies" or, more properly, damping rates. All symbols refer to depolarised light, except the inverted triangles, or nablas, which we shall discuss later. Frequencies are plotted *versus* the square of the wavevector **q**. Amongst all, twist data (circles) show the most evident diffusive behaviour, and fit reasonably well to a straight line passing by the origin, according to equation (4), giving $D_{twist} = 0.42 \times 10^{-12}\,\mathrm{m}^2\,\mathrm{s}^{-1}$.

The extrapolation to zero frequency as $q \to 0$ needs to be justified. Although not being rigorously true for depolarised light, it can be done here as a good approximation

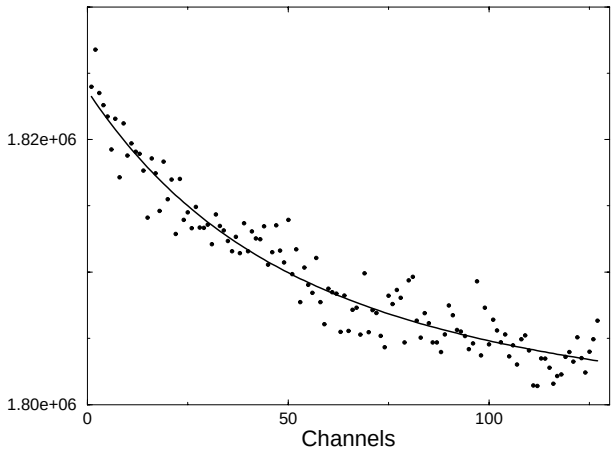

Fig. 8. Example of polarised residual signal obtained in a ideally forbidden geometry (see text) ($q_2 = 3.49 \times 10^6$ m^{-1}, $\Delta\tau = 20$ ms).

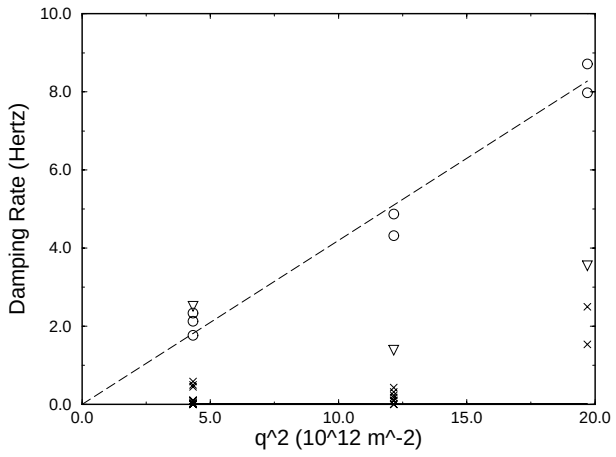

Fig. 9. Low frequency damping rate of fluctuations *versus* q^2: all symbols refer to depolarised light, except the nablas (∇). Crosses ($\times$) are long-time components, uninteresting for the present paper (see text).

for our lyotropic nematic system because of its weak birefringence [14] of $\Delta n \approx 2\times10^{-3}$. Thus the residual q_z component is $k_L\Delta n \approx 2 \times 10^4$ m^{-1}. This is comparable with the error bars of the optical wavevector setup (as a function of the scattering angle) and corresponds, in any case, to a negligible contribution to the relaxation frequency.

Now let us say a word about the lowest frequency data (crosses), which correspond to the long time component of the 2–exponential fit. They appear quite independent of q (if we ignore the apparent dependence shown by the q_3 points, probably "attracted" to the faster twist component, owing to a poor resolution). Such a non-diffusive charater is the signature of the already studied micellar mode [9]. Ordinarily, micellar fluctuations are expected to give only polarized scattering. However, they appear systematically in our depolarized signals too, as a weak component compared with the full (o, o) signal. This component may be due to polarization leakage, but it is also

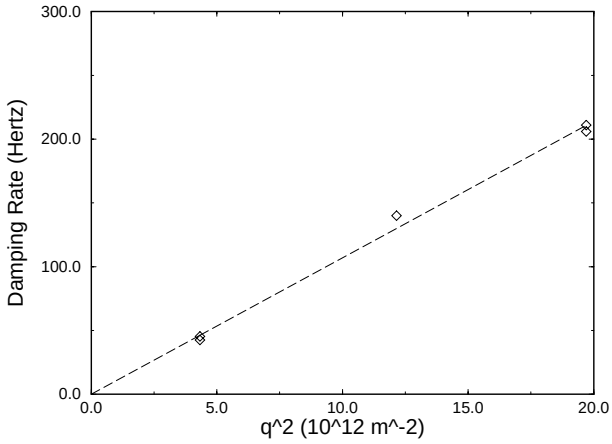

Fig. 10. High frequency damping rate of depolarized light signals (bend fluctuations) *versus* q^2.

possible to figure out mechanisms for micellar fluctuations giving rise to depolarized scattering [9]. Alternativelly, very slow convective disturbances also might generate long-time components. We shall not be concerned with these slow contributions here.

From the few data produced by turning the sample by 90° we obtain (see Fig. 10) $D_{bend} = 10.7 \times 10^{-12}$ m^{2}s^{-1}. This value is about three times lower than the one obtained for the phase N_C in reference [7]. Although the sample composition in the two experiments differs only slightly, the sample in that earlier one exhibited a biaxial nematic phase in neighbouring temperatures, which does not occur in the present experiment. Besides, the sample there, had not to be rotated, as **B** was applied parallel to **q**. Of course, the disturbance caused by such rotations may affect the precision of the present result for bend, in spite of the care taken in these operations.

Finally, let us discuss about the only polarised data appearing in Figure 9, the nablas. As we have said before, these (e, e) signals are residuals of a forbidden mode, issued of a mixture of splay and twist. In particular, the high wavevector data seem very influenced by the low frequency micellar mode. However, the q_1 data is higher, appearing together with the (depolarised) twist data. Although the poor quality of these (e, e) signals, they give evidence that splay and twist fluctuations relax with nearly the same characteristic times. Therefore we conclude that the backflow effect for splay in this N_C phase is negligible.

Taking this last isolated point as an estimate for the splay diffusivity, it gives roughly 0.5×10^{-12} m^{2}s^{-1}.

4 Comparative discussions and conclusion

Table 1 is a compilation of orientational diffusivity data for different nematic phases and geometrical configurations available in the literature. Lyotropic data include contributions of the present publication, some of the already mentioned previous ones on the LDhW system, and results of Čopič *et al.* [15] for a different lyotropic system.

Table 1. Orientational diffusivity coefficients corresponding to calamitic (N_C) and disk-like (N_D) nematic phases of lyotropic systems and to a classical rod-like system (MBBA).

	Lyotropic N_C phase of LDhW, [present paper] $T = 29.4\,^\circ$C	Lyotropic N_D phase of LDhW, Ref. [3] $T = 19\,^\circ$C	Lyotropic N_D phase of DHCDhW, Ref. [15] $T = 22\,^\circ$C	MBBA Ref. [1] $T = 25\,^\circ$C
D_{splay} (m^2s^{-1})	$\sim 0.5 \times 10^{-12}$	11.5×10^{-12}	4.5×10^{-12}	56×10^{-12}
D_{twist} (m^2s^{-1})	0.42×10^{-12}	1.6×10^{-12}	0.30×10^{-12}	43×10^{-12}
D_{bend} (m^2s^{-1})	10.7×10^{-12}	-	0.33×10^{-12}	430×10^{-12}
D_{splay}/D_{twist}	~ 1	7.2	15	1.3
D_{bend}/D_{twist}	25	1?	1.1	10

In addition, results for a classical nematic (MBBA) made of rod-like molecules are shown, for comparison.

As far as we know, this compilation gives an essentially complete picture of the diffusivity data presently available for lyotropic nematics. As a general conclusion, one can say that these data are quite consistent with the backflow model.

In particular, both the confirmation given here that $D_{bend} \gg D_{twist}$ (as a fact independent of the occurrence of the biaxial phase) and the additional information that $D_{splay} \approx D_{twist}$, bring new evidences to favour the hypothesis of interchange of the role of disks and cylinders between the phases N_C and N_D (see Fig. 3), as it was pointed out in reference [3]. In fact, the data presented here is complementary to those of that reference, and practically confirm the main predictions expected from the backflow model.

However, there remain some checks worth making. In the case of the LDhW system, they are presently limited by the lack of information in two fronts. First, the orientational diffusivity constant D_{bend} for the N_D phase. This quantity was not determined in reference [3] due to experimental limitations. Still, photocorrelation tests made with oblique geometries (regarding q and n_o) in that phase, gave no evidence of a high frequency depolarised component, which suggests the hypothetical "1?" that appears in the table. Moreover, this feature was already demonstrated for a different lyotropic system [15], which possesses a disk-like nematic phase of *positive* diamagnetic susceptibility. This somewhat exotic detail is very convenient to probe bend fluctuations of a discotic material by light scattering, allowing to establish that $D_{bend} \approx D_{twist}$ for the N_D phase of this system, as it can be seen in the table.

Second, the elastic constants of the LDhW system are not still precisely known. Although this information would improve the quantitative aspects of the problem, it is known from related lyotropic systems [16,17] that the ratio between the elastic constants is usually lower than a factor of two. So, it is hard to think of this as a decisive test for the backflow model.

Concerning other lyotropic systems, available data are rather scarce. In part, because there are not that many systems presently known which present nematic phases. The quoted light scattering measurements by Čopič *et al.* [15] were done on a five components system (a mixture of potassium decanoate potassium heptyloxybenzoate, potassium chloride, decanol and heavy water – referred in Tab. 1 as DHCDhW), which presents no other nematic phase than the N_D. As another example, let us mention a NMR study [17] on the system sodium dodecyl sulphate/decanol/water. Although these measurements do not discriminate the deformations (and so, are not suitable for a backflow analysis), they also give the orientational diffusivities for the N_D and N_C phases within the same range as those shown in Table 1.

Beyond lyotropics, on the other hand, the reader may recall that we made reference in the introduction to recent data on a thermotropic discotic material [5] that would behave at variance to the backflow mechanism. If such behaviour is confirmed, it opens new interesting questions on the subject of orientational diffusivities in nematics. The apparent lack of backflow effect verified by these authors, however, might be intrinsic of their thermotropic system, and does not invalidate our conclusion stated above. Furthermore, in a more recent publication [18] the same authors invoke a structural peculiarity which could be responsible by their observed result, namely the local positional order of disks (*i.e.*, the disks would make short "piles", or pseudo-rods, yielding a rod-like dynamical behaviour). This could explain a D_{splay}/D_{twist} ratio of the order of one and a relatively high ratio (of about three) for D_{bend}/D_{twist}. Although weaker, it is a behaviour somewhat like the one expected for rod-like nematics.

A final discussion is worth making recalling the controversy concerning the actual shape of the building blocks which constitute the different lyotropic nematic phases [19,20]. The basic question here is whether the shape of the micelles changes, for instance, from disks

to cylinders [20], according the phase is N_D or N_C. Another line of thinking claims [19] that all the three possible nematic phases (including the biaxial phase, N_B) share the same, unchanged, biaxial blocks, and so the different phases would be merely the result of their different forms of organisation.

In this connection, we should note from Table 1 that this last viewpoint is hard to conciliate with the ratios $D^C_{bend}/D^C_{twist} = 25$ and $D^D_{splay}/D^D_{twist} = 7.2$ obtained for the phases N_C and N_D, respectively, of the potassium laurate/decanol/heavy water mixture. The reason for that can be argued more simply within the single elastic constant approximation adopted above, that is, attributing the whole effect only to viscosities.

Then, if one visualises the N_C phase as oriented rods of length L and thickness a dispersed in a liquid of averaged viscosity η, one can, following Helfrich [21], estimate $\gamma_1 \sim (L/a)^2$. This argument can be extended [3] to disks of diameter D and thickness a, yielding $\gamma_1 \sim (D/a)^3$. Now, neutron [6] and X-rays [19] measurements give an estimate for the form factor $D/a \sim 2.2$. Concerning the determination of such structural parameters it is worth noting that while the bilayer thickness a is rather precisely known (≈ 26 Å), the other dimensions turn out to be far less well-defined.

Thus, these estimates suggest that the backflow is able to reduce the effective viscosity in the N_D phase from about $\gamma_1 \sim 10\eta$ down to η, which agrees reasonably with data shown in Table 1. Here comes the point, concerning structure. Such scaling behaviour for γ_1 makes difficult to understand the result $D^C_{bend}/D^C_{twist} > D^D_{splay}/D^D_{twist}$, unless, of course, if one admits that L is significantly greater than D. This conjecture seems to favour a model admitting shape change of the micelles between the two uniaxial nematic phases. However, it does not necessarily exclude the invariant shape model, provided the anisotropy of the (biaxial) objects is sufficiently high. This, however, seems not to be the case, according to the structural evidence presently known.

It is a pleasure to thank S.M. Freitas, E.M.A. Siqueira *et al.* from the Biophysics Laboratory at Universidade de Brasilia, for their kind assistance with sample preparations. We are also indebted to to O. Portilho and P.H. Acioli for valuable computational help and to Professor H. Gallardo from Santa Catarina University for providing us with purified K-laurate. Thanks are also due to the referee, for very helpful criticisms. Finally, M.A.A. thanks CNPq (brazilian government) for financial support.

References

1. P.G. de Gennes, *The Physics of Liquid Crystals* (Clarendon Press, Oxford, 1974), Chaps. 3 and 5.
2. Orsay Group on Liquid Crystals, Phys. Rev. Lett. **22**, 1361 (1969).
3. M.B. Lacerda Santos, Y. Galerne, G. Durand, J. Phys. France **46**, 933 (1985).
4. S. Fraden, R. Meyer, Phys. Rev. Lett. **57**, 3122 (1986).
5. T. Othman, M.M. Jebari, A. Gharbi, G. Durand, Liq. Cryst. **18**, 839 (1995).
6. Y. Hendrikx, J. Charvolin, M. Rawiso, L. Liébert, M.C. Holmes, J. Phys. Chem. **87**, 3991 (1983).
7. M.B. Lacerda Santos, G. Durand, J. Phys. France **47**, 529 (1986).
8. L.J. Yu, A. Saupe, Phys. Rev. Lett. **45**, 1000 (1980).
9. M.B. Lacerda Santos, W.B. Ferreira, M.A. Amato, Liq. Cryst. **16**, 287 (1994).
10. B.J. Berne, R. Pecora, *Dynamic Light Scattering* (Wiley, New York, 1976).
11. M.B. Lacerda Santos, Rev. Fis. Aplic. Instr. **7**, 1 (1992) (*in Portuguese*).
12. F.G. Jota, A.R. Braga, M.B. Lacerda Santos, Meas. Sc. Technol. **3**, 643 (1992).
13. M. Delaye, Ph.D. thesis, Orsay, 1978.
14. Y. Galerne, J.P. Marcerou, Phys. Rev. Lett. **51**, 2109 (1983).
15. M. Čopič, T. Ovsenik, M. Zgonik, Liq. Cryst. **2**, 643 (1987).
16. E. Zhou, M. Stefanov, A. Saupe, J. Chem. Phys. **88**, 5137 (1988).
17. B. Halle, P.-O. Quist, I. Furó, Phys. Rev. A **45**, 3763 (1992).
18. T. Othman, M.M. Jebari, A. Gharbi, G. Durand, Mol. Cryst. Liq. Cryst. **281**, 145 (1996).
19. A.M. Figueiredo Neto, Y. Galerne, L. Liébert, Liq. Cryst. **10**, 751 (1991).
20. J.P. McClymer, C.A. Oxborrow, P.H. Keyes, Phys. Rev. A **42**, 3449 (1990).
21. W. Helfrich, J. Chem. Phys. **50**, 100 (1969).